

Singapore Management University

## Institutional Knowledge at Singapore Management University

---

Research Collection School Of Economics

School of Economics

---

1-2002

### Monitoring process variability with symmetric control limits

Zhenlin YANG

*Singapore Management University*, [zlyang@smu.edu.sg](mailto:zlyang@smu.edu.sg)

Follow this and additional works at: [https://ink.library.smu.edu.sg/soe\\_research](https://ink.library.smu.edu.sg/soe_research)



Part of the [Econometrics Commons](#)

---

#### Citation

YANG, Zhenlin. Monitoring process variability with symmetric control limits. (2002). 1-22.

Available at: [https://ink.library.smu.edu.sg/soe\\_research/2064](https://ink.library.smu.edu.sg/soe_research/2064)

This Working Paper is brought to you for free and open access by the School of Economics at Institutional Knowledge at Singapore Management University. It has been accepted for inclusion in Research Collection School Of Economics by an authorized administrator of Institutional Knowledge at Singapore Management University. For more information, please email [cherylds@smu.edu.sg](mailto:cherylds@smu.edu.sg).

See discussions, stats, and author profiles for this publication at: <https://www.researchgate.net/publication/301683311>

# Monitoring process variability with symmetric control limits

Article · January 2002

---

CITATIONS

0

---

READS

11

1 author:



Zhenlin Yang

Singapore Management University

94 PUBLICATIONS 660 CITATIONS

SEE PROFILE

All content following this page was uploaded by [Zhenlin Yang](#) on 28 April 2016.

The user has requested enhancement of the downloaded file. All in-text references [underlined in blue](#) are added to the original document and are linked to publications on ResearchGate, letting you access and read them immediately.

# Monitoring Process Variability with Symmetric Control Limits

ZHENLIN YANG<sup>1\*</sup> and MIN XIE<sup>2</sup>

<sup>1</sup>*School of Economics and Social Sciences, Singapore Management University, and*

<sup>2</sup>*Department of Industrial and Systems Engineering, National University of Singapore*

## Abstract

Control charts for monitoring process variability, such as the R-chart and  $S$ -chart, do not have symmetric probability limits as the distribution of the sample variability is not normal. Hence, the usual zone rules can not be applied although it is still desirable to be able to use the information from more than one point in decision making. In this paper, a modified  $S$ -chart based on an optimal normalizing transformation of the sample variance is first introduced. The new chart is shown to have approximate symmetric probability limits and hence can be interpreted in the same way as that of a  $\bar{X}$  chart. This modified chart is shown to be comparable with the probability  $S$ -chart and have a much better performance than the usual Shewhart  $S$ -chart for the cases of known and estimated limits. The effect of parameter estimation is investigated. The optimal normalizing transformation is a simple power transformation. The power parameter depends only on the sample size and approaches  $1/3$  as the sample size increases. Hence, the transformation  $S$ -chart can be easily implemented and integrated into any SPC system.

---

\*Correspondence: School of Economics and Social Sciences, Singapore Management University, 469 Bukit Timah Road, Singapore 259756 Tel.: (65) 6822-0852, fax: (65) 6833-0833, email: zlyang@smu.edu.sg

## 1 Introduction

Statistical process control techniques, especially the  $\bar{X}$  and *R*-charts, are widely used in manufacturing industry today (Elsayed, 2000). The process is deemed to be out-of-control when a point falls outside the control limits. However, as the control chart is a display of the information in sequence, any non-normal pattern can also be very informative. The so-called zone rules have been developed to make use of more than a single point in the decision making (Western Electric, 1956, Nelson, 1984, Parkhideh and Parkhideh, 1996, etc.).

Usually the zone rules are considered to be applicable only for the  $\bar{X}$  chart under the normality assumption. It is not considered to be useful for the traditional *R*-chart or *S*-chart when monitoring process variability although the idea of using the information from more than one point should be applicable as well. A reason for that is that *R*-chart or *S*-chart is a plot of quantities that are highly non-normal. Hence, the interpretation based on zone rules would not be the same as for the  $\bar{X}$  chart.

Data non-normality is a common problem in statistical process control. For non-normal quantities, a simple method is to transform the data to normal. Such studies have been reported for direct observations (Nelson, 1994, [Kittlitz, 1999](#), and Xie et al. 2000). However, the chart for monitoring the mean is based on the average from a sample of fixed size. The effect of non-normality is less serious for sample average than individual measurement. For chart for variability, on the other hand, only single value is available, and non-normality is a problem.

In this article, we consider a transformation approach to develop a nearly normal-based control chart for monitoring process variability. It is well known that the variance of a normal sample is related to a chi-squared random variable that is transformable to near normality by a simple power transformation (Hernandez and Johnson, 1981, Hawkins and Wixley, 1986). Thus, a control chart for the transformed sample variance can be constructed in the traditional way. When necessary, the control limits can be back-transformed to give a control chart for the sample standard deviation or the sample

variance itself. In this paper, we will focus on the *S*-chart as it is a better measure of process variability and it is especially useful when the sample size is of moderate size. The *S*-chart is also relatively simple compared with other more cusum or ewma based charts ([Acosta-mejia et al., 1999](#)).

The optimal transformation proposed here is obtained based on the measure of Kullback-Leibler information number (Kullback, 1968). It is shown that the power of the transformation depends only on the sample size and that if the sample size is large enough ( $\geq 5$ , say), the power can simply be taken as  $1/3$ , a very convenient number that can simply be handled by a pocket calculator. A table of optimal transformation values as well as the mean and standard deviation of the transformed chi-squared variable is provided to assist the construction of the transformation *S*-chart.

The performance of the transformation *S*-chart is studied and compared with both the classical Shewhart *S*-chart and the *S*-chart with probability limits. It is found that the transformation *S*-chart is comparable with the probability *S*-chart and has a better performance than the Shewhart *S*-chart. Section 2 outlines the Shewhart and Probability *S*-charts. Section 3 introduces the transformation *S*-chart. Section 4 presents an illustrative example. The alarm probabilities and the run length distributions of the three charts are studied and compared in Section 5 and 6. Both the cases of known limits and estimated limits are considered.

## 2 The Shewhart and Probability *S*-Charts

Traditional ways of monitoring the process variability are through *S*-,  $S^2$ - or *R*-chart, which could be either the Shewhart type or charts with probability limits. Detailed accounts for these charts can be found in, for examples, Montgomery (1997) and Quesenberry (1997). Let  $X_1, X_2, \dots, X_n$  be a random sample from  $N(\mu, \sigma^2)$ . Let  $S^2$  be the sample variance and  $S$  the sample standard deviation. The control limits for a classical Shewhart *S*-chart for monitoring the process standard deviation  $\sigma$  are given

by:  $UCL_C = \sigma_0 (c + k\sqrt{1 - c^2})$ ,  $CL_C = \sigma_0 c$  and  $LCL_C = \sigma_0 (c - k\sqrt{1 - c^2})$ . and the assumption is that the distribution of  $S$  can be approximated by normal, where

$$c = \frac{\Gamma(n/2)}{\Gamma[(n-1)/2]} \sqrt{\frac{2}{n-1}},$$

When the true process standard deviation  $\sigma_0$  is unknown, a common practice is to estimate it based on the past data and treat the estimate as if it is the true value. Suppose we have  $m$  samples of in-control data of size  $n$  each. Let  $S_i$  be the standard deviation of the  $i$ th sample,  $i = 1, 2, \dots, m$ . The usual estimators of  $\sigma_0$  are either  $\bar{S}$ , the average of the sample standard deviations, or the pooled estimator

$$S_p = \sqrt{\frac{n-1}{nm-m} \sum_{i=1}^m S_i^2}.$$

The latter is specifically recommended for the case of unequal sample sizes (Quesenberry, 1997, p180). We adopt the  $S_p$  estimator as the square of it is related to a chi-square distribution. Replacing  $\sigma_0$  by  $S_p$  gives the Shewhart  $S$ -chart with estimated control limits:

$$\begin{aligned} \widehat{UCL}_C &= S_p(c + k\sqrt{1 - c^2}), \\ \widehat{CL}_C &= S_p c \\ \widehat{LCL}_C &= S_p(c - k\sqrt{1 - c^2}). \end{aligned} \tag{1}$$

It should be noted that the properties of the chart (1) has not been studied. In particular, how large the  $m$  has to be so that the chart performs as if  $\sigma$  is given. This issue will be addressed in the latter section together with the newly introduced chart.

Now, based on the distributional result for the variance of a normal sample, one can easily construct an  $S$ -chart with exact probability limits:  $UCL_P = \sigma_0 \sqrt{\chi_{n-1}^2(\alpha_l)/(n-1)}$ ,  $CL_P = \sigma_0 \sqrt{\chi_{n-1}^2(0.5)/(n-1)}$ , and  $LCL_P = \sigma_0 \sqrt{\chi_{n-1}^2(\alpha_u)/(n-1)}$ , where  $\chi_{\nu}^2(\alpha)$  is the upper  $\alpha$ th percentile of a chi-squared random variable with  $\nu$  degrees of freedom. When  $\sigma_0$  is unknown and is replaced by  $S_p$ , we have the probability  $S$ -chart with estimated control limits:

$$\widehat{UCL}_P = S_p \sqrt{\chi_{n-1}^2(\alpha_l)/(n-1)}$$

$$\begin{aligned}\widehat{CL}_P &= S_p \sqrt{\chi_{n-1}^2(0.5)/(n-1)} \\ \widehat{LCL}_P &= S_p \sqrt{\chi_{n-1}^2(\alpha_u)/(n-1)}.\end{aligned}\tag{2}$$

Chen (1998) has studied the properties of (2) and concluded that when compared to the charts with known  $\sigma$ , the charts with estimated  $\sigma$  signal more often when the process is stable and do not signal as quickly when the process variability has changed.

### 3 The Transformation S-Chart

It is well known that the basic requirement for the application of the zone rules is that the quantity to be plotted on the chart is normally distributed, so that the probabilities for a point to fall into respective zones when the process is stable are 0.00135, 0.02145, 0.13590, 0.34130, 0.13580, 0.02145 and 0.00135. The cutoff points for the zones are defined as  $\mu^* \pm k\sigma^*$ ,  $k = 1, 2, 3$ , where  $\mu^*$  and  $\sigma^*$  are, respectively, the expectation and standard deviation of the plotted quantity. These rule are certainly not applicable to the usual S-charts as the distribution of the sample standard deviation is not normal.

Although the zone tests are normally not recommended for the charts for monitoring the process variability, in many cases the chart users still interpret it in such a way. In fact, the primary reason why the zone rules should not be used is the non-normality of S-chart. It would be useful to have a chart that provides symmetry control limits, so that the chart can be interpreted as others. For example, when many points fall on one side of the control chart, the chart user can be alarmed and assignable causes can be found. We now introduce the so called transformation S-chart. The idea is that if a quality measure is not normal, it may be transformable to near normality by a simple power transformation. A Shewhart chart can be constructed for the normalized quality and the zone rule can be applied.

Since  $(n-1)S^2/\sigma \sim \chi_{n-1}^2$ , which is a special gamma with scale parameter 2 and shape parameter  $\tau = (n-1)/2$ , the normalizing transformation results for the gamma distribution outlined in the Appendix are thus applicable. Let  $Y = [(n-1)S^2/\sigma^2]^{\lambda_0}$ ,

where  $\lambda_0$  is the optimal transformation parameter, then  $Y$  is approximate normal with mean and standard deviation:

$$\mu(\lambda_0) = 2^{\lambda_0} \frac{\Gamma(\tau + \lambda_0)}{\Gamma(\tau)} \text{ and } \sigma(\lambda_0) = 2^{\lambda_0} \sqrt{\frac{\Gamma(\tau + 2\lambda_0)}{\Gamma(\tau)} - \frac{\Gamma^2(\tau + \lambda_0)}{\Gamma^2(\tau)}},$$

All three quantities,  $\lambda_0$ ,  $\mu(\lambda_0)$  and  $\sigma(\lambda_0)$ , depend purely on  $n$  or the shape parameter of the gamma distribution. Table 1 summarizes these values.

Table 1: A Summary of Transformation Values

$n$	$\lambda_0$	$\mu(\lambda_0)$	$\sigma(\lambda_0)$	$n$	$\lambda_0$	$\mu(\lambda_0)$	$\sigma(\lambda_0)$
2	0.20831	0.83766	0.30540	22	0.32764	2.68310	0.27418
3	0.26543	1.08583	0.32156	23	0.32791	2.72786	0.27244
4	0.28843	1.27938	0.32424	24	0.32815	2.77124	0.27077
5	0.30027	1.43689	0.32239	25	0.32838	2.81332	0.26916
6	0.30733	1.57021	0.31900	26	0.32858	2.85421	0.26763
7	0.31197	1.68640	0.31515	27	0.32877	2.89399	0.26615
8	0.31523	1.78983	0.31127	28	0.32894	2.93272	0.26472
9	0.31764	1.88340	0.30752	29	0.32910	2.97047	0.26335
10	0.31950	1.96908	0.30396	30	0.32925	3.00731	0.26203
11	0.32096	2.04832	0.30060	31	0.32939	3.04328	0.26075
12	0.32215	2.12217	0.29745	32	0.32952	3.07844	0.25951
13	0.32313	2.19145	0.29448	33	0.32964	3.11282	0.25832
14	0.32395	2.25679	0.29169	34	0.32976	3.14647	0.25716
15	0.32466	2.31870	0.28907	35	0.32987	3.17943	0.25604
16	0.32526	2.37759	0.28659	36	0.32997	3.21173	0.25495
17	0.32579	2.43380	0.28425	37	0.33006	3.24341	0.25389
18	0.32625	2.48761	0.28203	40	0.33032	3.33494	0.25089
19	0.32666	2.53925	0.27992	60	0.33135	3.84720	0.23559
20	0.32702	2.58894	0.27791	100	0.33214	4.59053	0.21720
21	0.32735	2.63684	0.27600	200	0.33274	5.81358	0.19415

Note:  $\lambda_0 \rightarrow 1/3$  as  $n \rightarrow \infty$ .

Now, based on the above arguments, an approximate  $k$ -sigma control chart for  $Y$  can be readily constructed with control limits:  $UCL = \mu(\lambda_0) + k\sigma(\lambda_0)$ ,  $CL = \mu(\lambda_0)$ , and  $LCL = \mu(\lambda_0) - k\sigma(\lambda_0)$ , which can easily be converted to a control chart for  $S^{2\lambda_0}$ :

$$\begin{aligned} UCL_T &= \nu_0[\mu(\lambda_0) + k\sigma(\lambda_0)], \\ CL_T &= \nu_0\mu(\lambda_0), \\ LCL_T &= \nu_0[\mu(\lambda_0) - k\sigma(\lambda_0)], \end{aligned} \tag{3}$$

where  $\nu_0 = [\sigma_0^2/(n-1)]^{\lambda_0}$ .



The control chart given by (3) is termed in this article the **transformation *S*-chart**. As the distribution of the plotted quality,  $S^{2\lambda_0}$ , is approximate normal, the usual zones rules can be applied. When  $\sigma_0$  is unknown and is estimated by  $S_p$ , the resulted transformation *S*-chart with estimated control limits has the form:

$$\begin{aligned}\widehat{UCL}_T &= \hat{\nu}_0[\mu(\lambda_0) + k\sigma(\lambda_0)] \\ \widehat{CL}_T &= \hat{\nu}_0\mu(\lambda_0) \\ \widehat{LCL}_T &= \hat{\nu}_0[\mu(\lambda_0) - k\sigma(\lambda_0)]\end{aligned}\tag{4}$$

where  $\hat{\nu}_0 = [S_p^2/(n-1)]^{\lambda_0}$

Notice that the implementation of the transformation *S*-chart remains very simple: the constants  $\lambda_0$ ,  $\mu(\lambda_0)$ , and  $\sigma(\lambda_0)$  are available from Table 1 and the quantity to be plotted  $S^{2\lambda_0}$  can be easily calculated by a pocket calculator once the  $S^2$  value is available. Notice also that when it is necessary, the transformation *S*-chart can easily be back transformed to give an *S*-chart or  $S^2$  chart.

There are two major issues needed to be addressed concerning the transformation *S*-chart: i) the performance of this chart relative to the usual Shewhart and probability *S*-chart and ii) the effect of estimating control limits on the performance of the transformation *S*-chart. We will address these two issues jointly latter after presenting an illustrative example.

## 4 An Example

The Wrist Pin Diameter data given by Quesenberry (1997, p 186) is considered here for illustrating the application of the transformation *S*-chart. There appear to be two misprints in the original data: the third observations for samples 20 and 37. It appears to be that the correct values should be 0.9987 and 0.9998 instead of 0.0998 and 0.0998. We follow the stage 2 analysis of Quesenberry, i.e., the sample 28 is deleted. The pooled estimator for  $\sigma$  based on 49 samples of size 5 each is  $S_p = 0.00122$ . Since  $n = 5$ , we

have  $\tau = (n - 1)/2 = 2$  and from Table 3, we obtain  $\lambda_0 = 0.30027$ ,  $\mu(\lambda_0) = 1.43689$ , and  $\sigma(\lambda_0) = 0.32239$ . Thus,  $\hat{\nu}_0 = [S_p^2/(n - 1)]^{\lambda_0} = 0.01173$  and the control limits for the transformation *S*-chart are:

$$\widehat{UCL}_T = \hat{\nu}_0[\mu(\lambda_0) + k\sigma(\lambda_0)] = 0.02820$$

$$\widehat{CL}_T = \hat{\nu}_0\mu(\lambda_0) = 0.01685$$

$$\widehat{LCL}_T = \hat{\nu}_0[\mu(\lambda_0) - k\sigma(\lambda_0)] = 0.00551$$

for  $k = 3$ . For  $k = 2$ , the upper and lower control limits are, respectively, 0.02442 and 0.00929. The transformation *S*-charts are plotted in Figure 1. The control limits for the transformation *S*-chart can easily be back-transformed to give control limits of a retransformed *S*-chart.

The estimated control limits for Shewhart *S*-chart are:  $\widehat{UCL}_C = 0.002399$ ,  $\widehat{CL}_C = 0.001112$  and  $\widehat{LCL}_C = 0.0$  for  $k = 3$ , and  $\widehat{UCL}_C = 0.001982$  and  $\widehat{LCL}_C = 0.000315$  for  $k = 2$ . The estimated control limits for the probability *S*-chart where  $\sigma$  is replaced by  $S_p$  are also calculated, which are:  $\widehat{UCL}_P = 0.002577$ ,  $\widehat{CL}_P = 0.001119$  and  $\widehat{LCL}_P = 0.000195$  for  $k = 3$ , and  $\widehat{UCL}_P = 0.002057$  and  $\widehat{LCL}_P = 0.000411$  for  $k = 2$ .

Note that the 3-sigma classical *S*-chart has a lower limit 0 and an upper limit that is significantly lower than that of the retransformed UCL of the transformation chart. This explains why the *S*-chart can give a high FAR and why it is insensitive to a decrease in process variability. Note also that the retransformed *S*-chart and the probability *S*-chart have almost identical control limits for  $k = 2$ . They are also very similar for the 3-sigma charts. For this reason, only the retransformed *S*-chart and Shewhart *S*-chart are constructed together in Figure 2.

It is interesting to see how the zone rules apply to *S*-chart and transformation *S*-chart. The estimated mean and standard deviation of  $S^{2\lambda_0}$  are:  $\hat{\nu}_0\mu(\lambda_0) = 0.01685$  and  $\hat{\nu}_0\sigma(\lambda_0) = 0.00378$ . The estimated mean and standard deviation of  $S$  are:  $cS_p = 0.00115$  and  $\sqrt{1 - c^2}S_p = 0.00042$ . The zone charts are given in Figure 3. It is clear that, if the process is stable, the transformation *S*-chart is more suitable when zone rules are used.

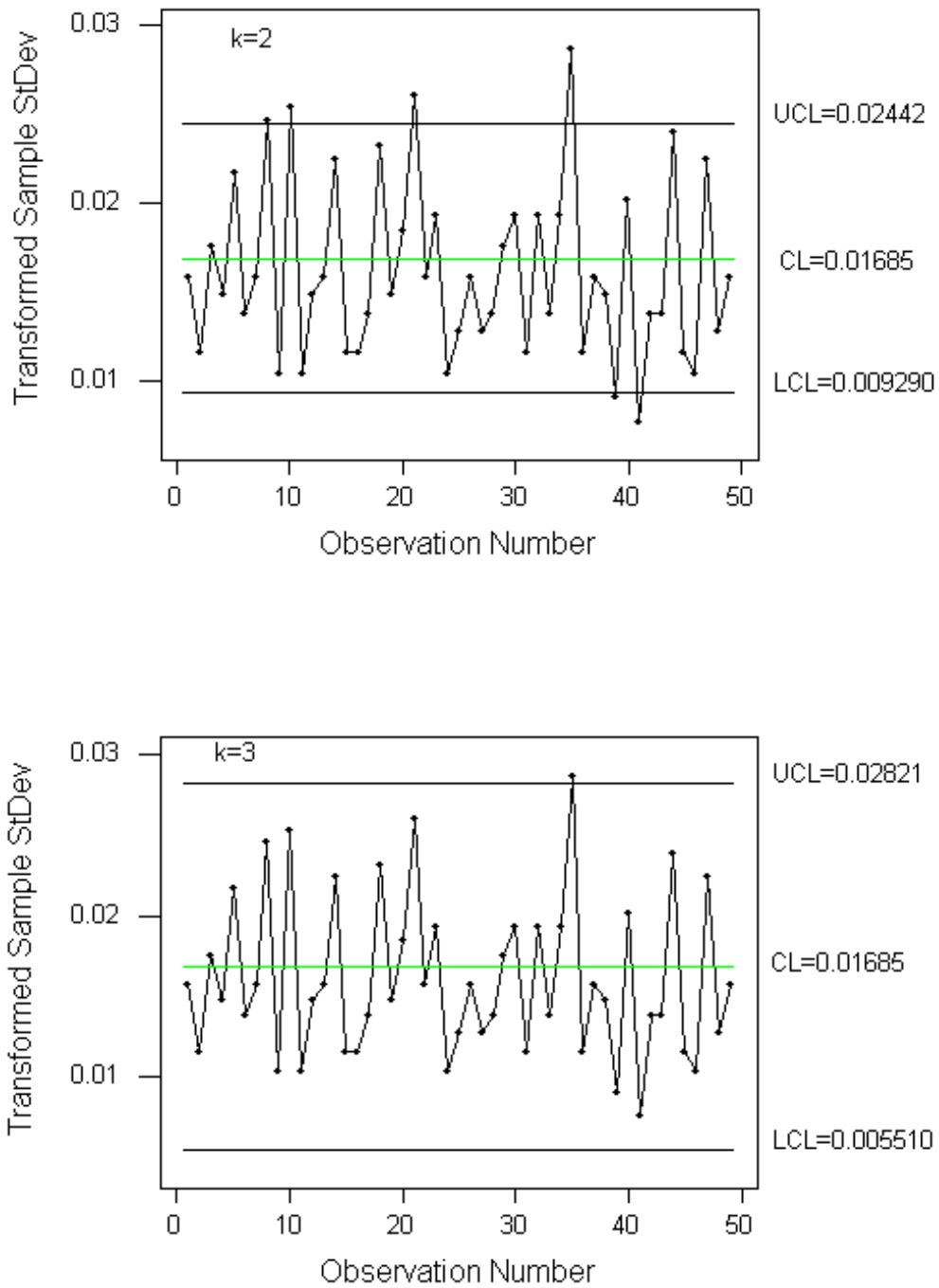


Figure 1: Transformation S-chart for the Wrist Pin Diameter Data

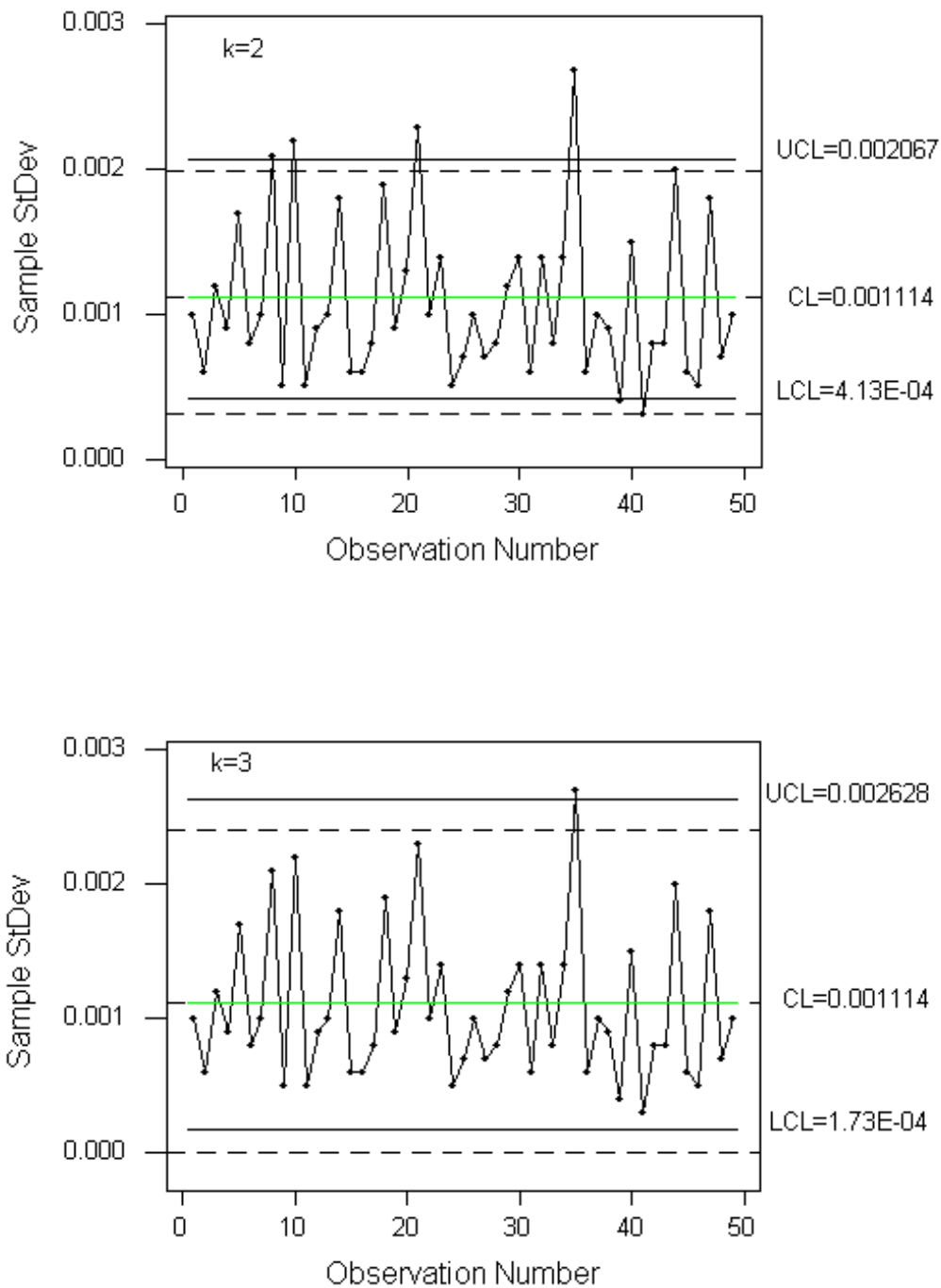


Figure 2: Retransformed (solid line) and Shewhart *S*-Charts for the Wrist Pin Diameter Data

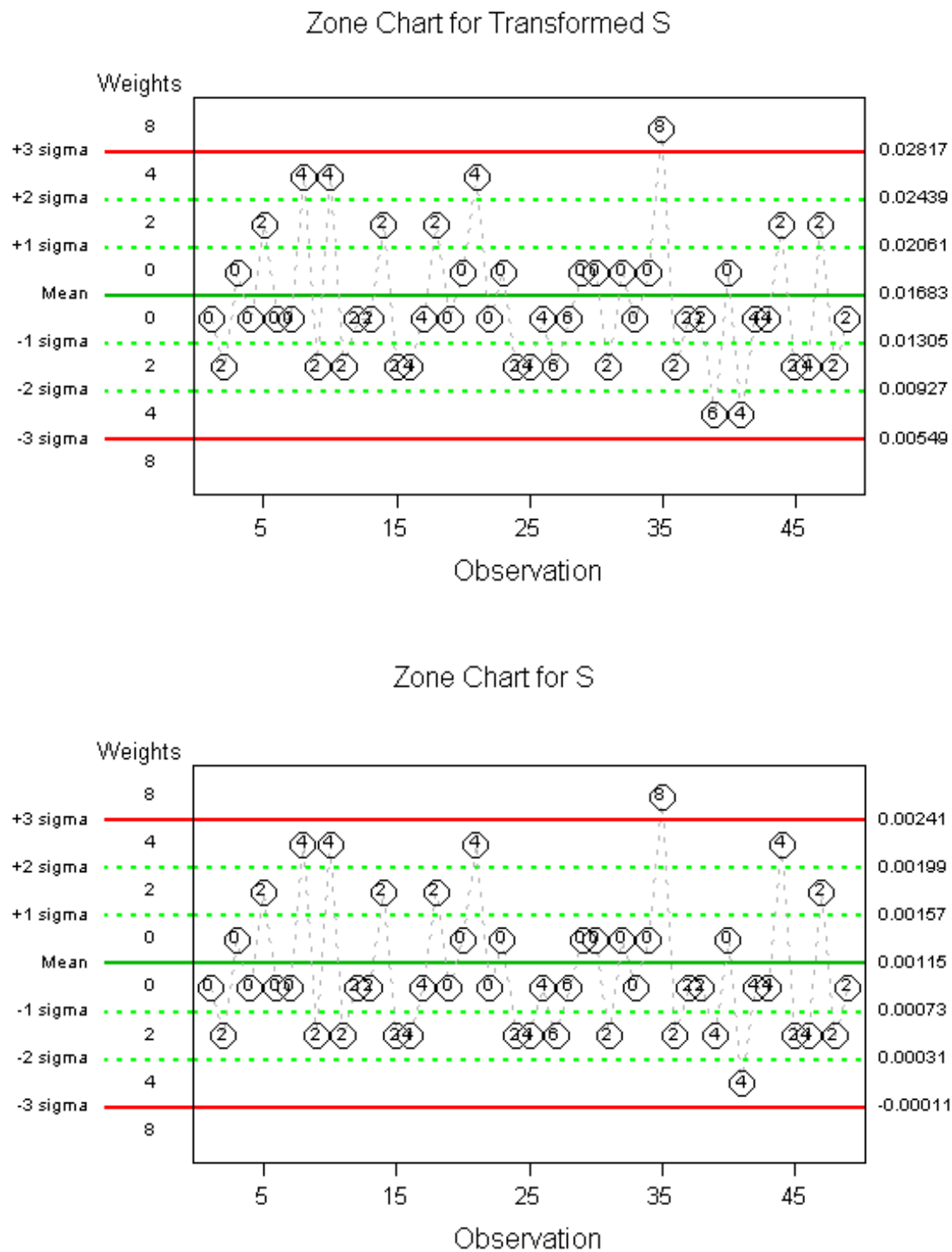


Figure 3: Zone Charts for  $S^{2\lambda_0}$  and  $S$ , the Wrist Pin Diameter Data

## 5 An Investigation of the Alarm Probability

The transformation  $S$ -chart is based on a simple power transformation with the power parameter depending only on the sample size. Hence it is easy to apply and the control limits are very close to the exact probability limits with an added advantage of having symmetric control limits. However, the chart properties have to be studied, for the case of a known model parameter and the case when the parameter is estimated. In this section, the traditional alarm probabilities are investigated and compared with the Shewhart  $S$ -chart and probability  $S$ -chart.

Let  $\sigma_0$  be the target (nominal) parameter value and  $\sigma = \delta\sigma_0$ ,  $\delta > 0$ , be the shifted parameter value. When the control limits are known, it is easy to see that the alarm probability (rate) for the transformation  $S$ -chart is:

$$\alpha_T^0(\delta) = 1 - G_{n-1}(U_T/\delta^2) + G_{n-1}(L_T/\delta^2), \quad (5)$$

where  $U_T = [\mu(\lambda_0) + k\sigma(\lambda_0)]^{1/\lambda_0}$ ,  $L_T = [\mu(\lambda_0) - k\sigma(\lambda_0)]^{1/\lambda_0}$ , and  $G_\nu(\cdot)$  denotes the cumulative distribution function (CDF) of a  $\chi_\nu^2$  random variable. When the control limits are estimated, the alarm rate becomes:

$$\alpha_T(\delta) = 1 - \mathfrak{S}_{N-m}^{n-1}[U_T/(\delta^2(n-1))] + \mathfrak{S}_{N-m}^{n-1}[L_T/(\delta^2(n-1))]. \quad (6)$$

where  $\mathfrak{S}_{N-m}^{n-1}(\cdot)$  denotes the CDF of an  $F_{n-1, N-m}$  random variable and  $N = nm$ . When  $\delta = 1$ , i.e., the process is in control, the above alarm rates become, respectively, the false alarm rates (FARs) for the  $S$ -chart with known or estimated control limits.

By comparing (6) with (5), it is not difficult to see that  $\alpha_T(\delta)$  is larger than  $\alpha_T^0(\delta)$  as the  $F_{n-1, N-m}$  random variable involved in calculating  $\alpha_T(\delta)$  is stochastically larger than the  $\chi_{n-1}^2/(n-1)$  random variable involved in calculating  $\alpha_T^0(\delta)$ . This says that estimating the control limits inflates the alarm rate. Similar conclusion holds for the probability  $S$ -chart (Chen, 1998) and the Shewhart  $S$ -chart.

Replacing  $U_T$  and  $L_T$  in (5) and (6) by  $\chi_{n-1}^2(\alpha_u)$  and  $\chi_{n-1}^2(1 - \alpha_l)$  gives the alarm rates for the probability  $S$ -chart, and by  $(n-1)[c + k\sqrt{1-c^2}]$  and  $(n-1)[c - k\sqrt{1-c^2}]$  gives the alarm rate for the Shewhart  $S$ -chart.

To compare the AR of the transformation *S*-chart with the ARs of the other two *S*-charts, we plot the operating characteristic (OC) functions of the three charts in Figures 4 and 5, where the OC function is defined as  $1 - \alpha(\delta)$ . From the plots we see that the transformation *S*-chart is comparable with the probability *S*-chart and has a better overall performance than the Shewhart *S*-chart, no matter whether the control limits are known or estimated. A careful comparison of Figure 5 with Figure 4 shows that estimating control limits indeed increases the FAR and decreases the AR when the process is shifted. This agrees with the qualitative conclusion reached above.

## 6 The Run Length Distribution

The run length (RL) is the number of samples required until an out-of-control signal is observed. Let  $R_T^0$  be the run length of the transformation *S*-chart when control limits are known and  $R_T$  be that when control limits are estimated. It is well known that the distribution of  $R_T^0$  is geometric with the probability of 'success' (an out-of-control signal)  $\alpha_T^0(\delta)$ . Hence, the corresponding average run length (ARL) and standard deviation of run length (SDRL) are, respectively,

$$ARL_T^0(\delta) = 1/\alpha_T^0(\delta) \text{ and } SDRL_T^0(\delta) = \sqrt{1 - \alpha_T^0(\delta)}/\alpha_T^0(\delta).$$

The RL distribution for the *S*-chart with estimated control limits can be obtained through some conditional arguments. Let  $S^0$  be a future sample standard deviation with the process standard deviation  $\sigma$  (or  $\sigma_0$  if the process standard deviation is not shifted). Define  $W = (N - m)S_p^2/\sigma_0^2$ . Thus,  $W$  is a  $\chi_{N-m}^2$  random variable and conditioning on  $S_p^2$  is equivalent to conditioning on  $W$ . It is easy to see that the conditional distribution of  $R_T$ , given  $W$ , is geometric with the conditional probability of an out-of-control signal:

$$\alpha_T(W) = 1 - G_{n-1} \left\{ \frac{WU_T}{\delta^2(N-m)} \right\} + G_{n-1} \left\{ \frac{WL_T}{\delta^2(N-m)} \right\}. \quad (7)$$

The unconditional distribution of  $R_T$  is thus,

$$f_{R_T}(r) = E \left\{ [1 - \alpha_T(W)]^{r-1} \alpha_T(W) \right\}, r = 1, 2, \dots \quad (8)$$

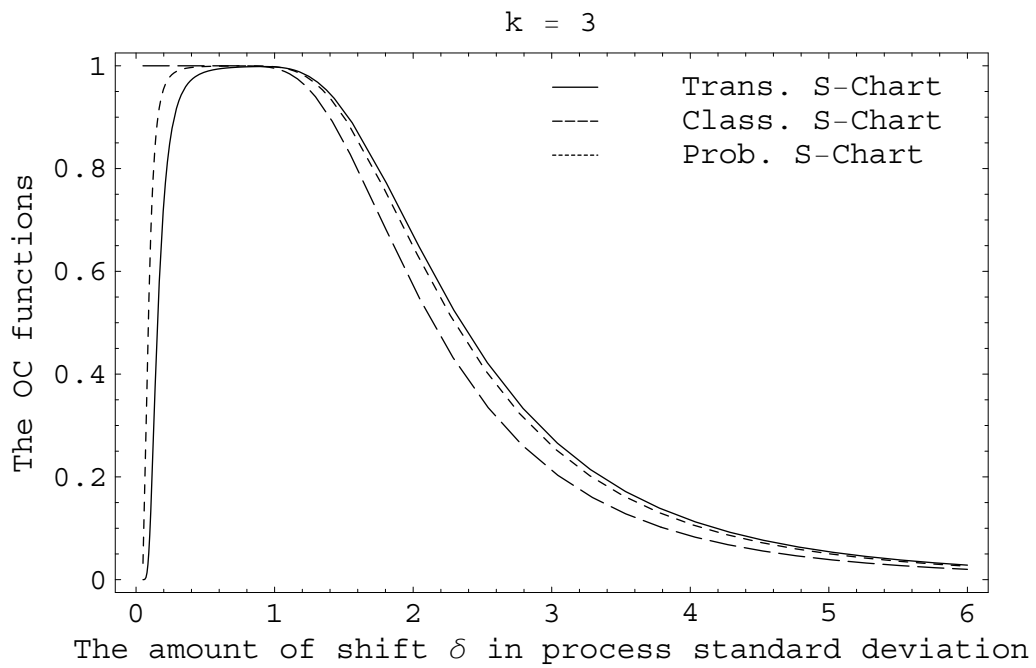
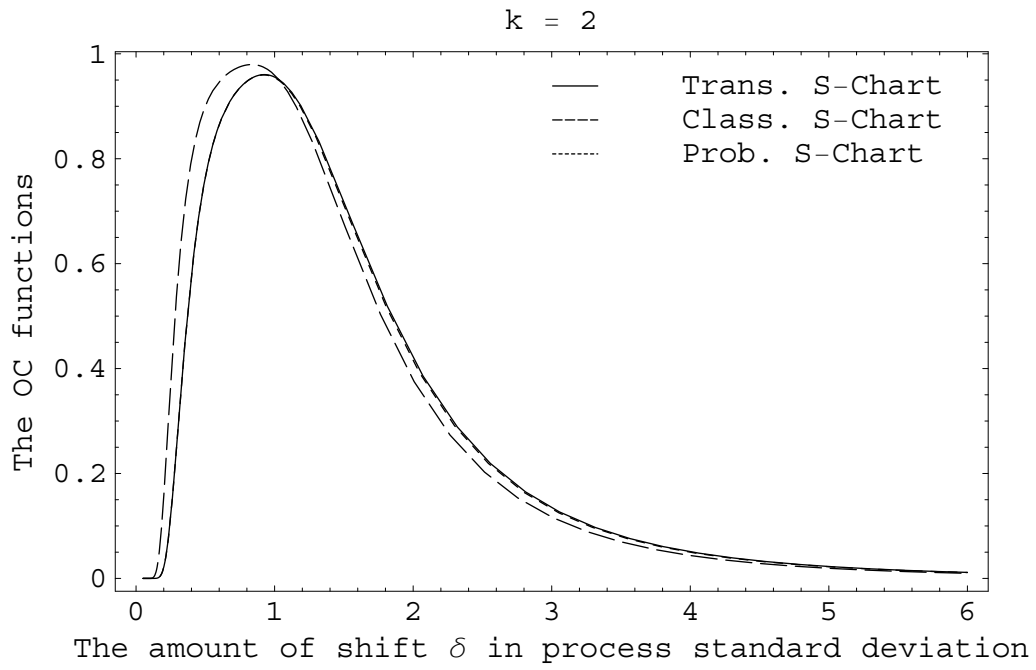


Figure 4: Plots of OC Functions:  $n = 5, m = \infty$



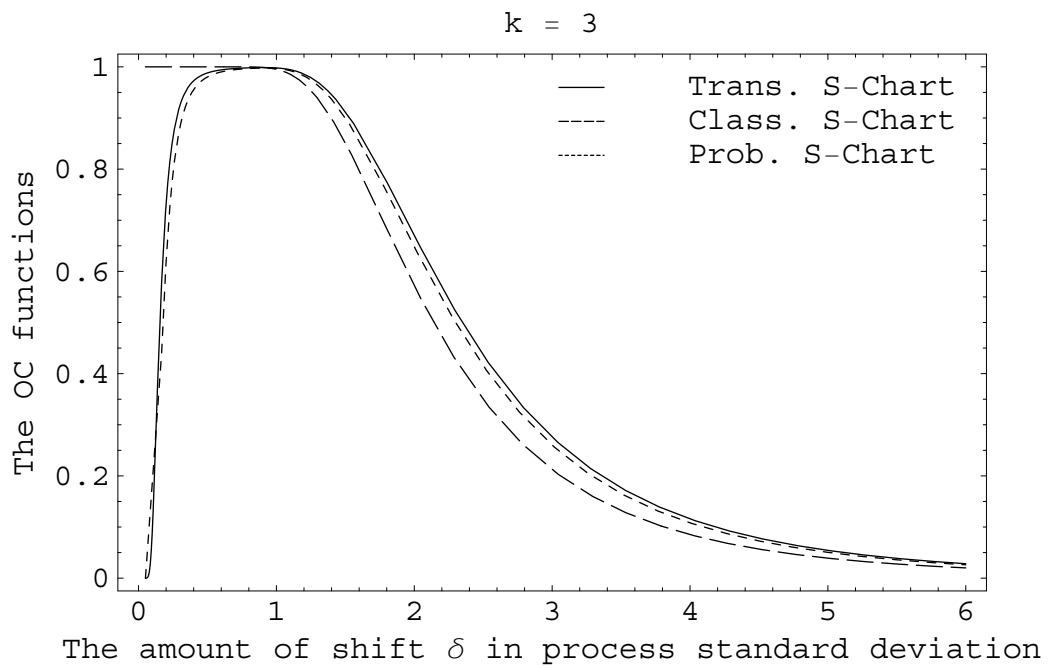
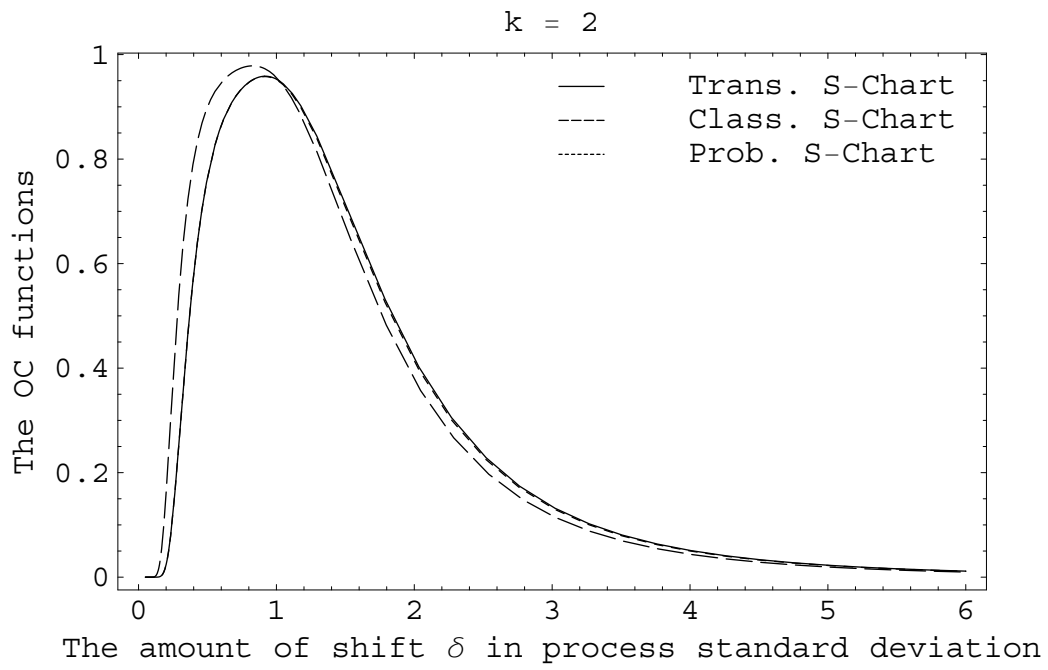


Figure 5: Plots of OC Functions:  $n = 5, m = 20$

with the ARL and SDRL given respectively as follows:

$$\begin{aligned} ARL_T(\delta) &= E[1/\alpha_T(W)] \text{ and} \\ SDRL_T(\delta) &= \sqrt{Var[1/\alpha_T(W)] + E[(1 - \alpha_T(W))/\alpha_T^2(W)]} \end{aligned}$$

Again, replacing  $U_T$  and  $L_T$  in (7) and (8) by  $\chi_{n-1}^2(\alpha_u)$  and  $\chi_{n-1}^2(1 - \alpha_l)$  gives the RL distribution for the probability *S*-chart with estimated limits, and by  $(n - 1)[c + k\sqrt{1 - c^2}]$  and  $(n - 1)[c - k\sqrt{1 - c^2}]$  gives the RL distribution for the Shewhart *S*-chart with estimated limits.

The three ARL functions are first plotted and compared in Figures 6 and 7. As the performance of the transformation *S*-chart is very close to the probability *S*-chart, the probability *S*-chart is not shown on the plots.

To illustrate the effect of estimating control limits on the performance of the transformation *S*-chart, the RL distribution of the transformation *S*-chart is plotted in Figure 8 for several different  $\delta$  values.

## 7 Discussions

It seems that there is an increasing trend in applying normalizing transformations to non-normal quality characteristics in SPC applications. See, for example, Nelson (1994), Chow, Polansky and Mason (1998), Kittlitz (1999), Yang and Xie (2000). and Shore (2000a, b). Measures of process variability, such as the sample variance, are non-normal, hence an application of a normalizing transformation can improve the validity of the control charts. The transformation approach for *S*-chart construction is attractive as the optimal transformation depends only the sample size. The gain of applying transformation is significant, especially when compared with the classical *S*-chart where the chart is constructed on the original sample standard deviation that is clearly far from normal.

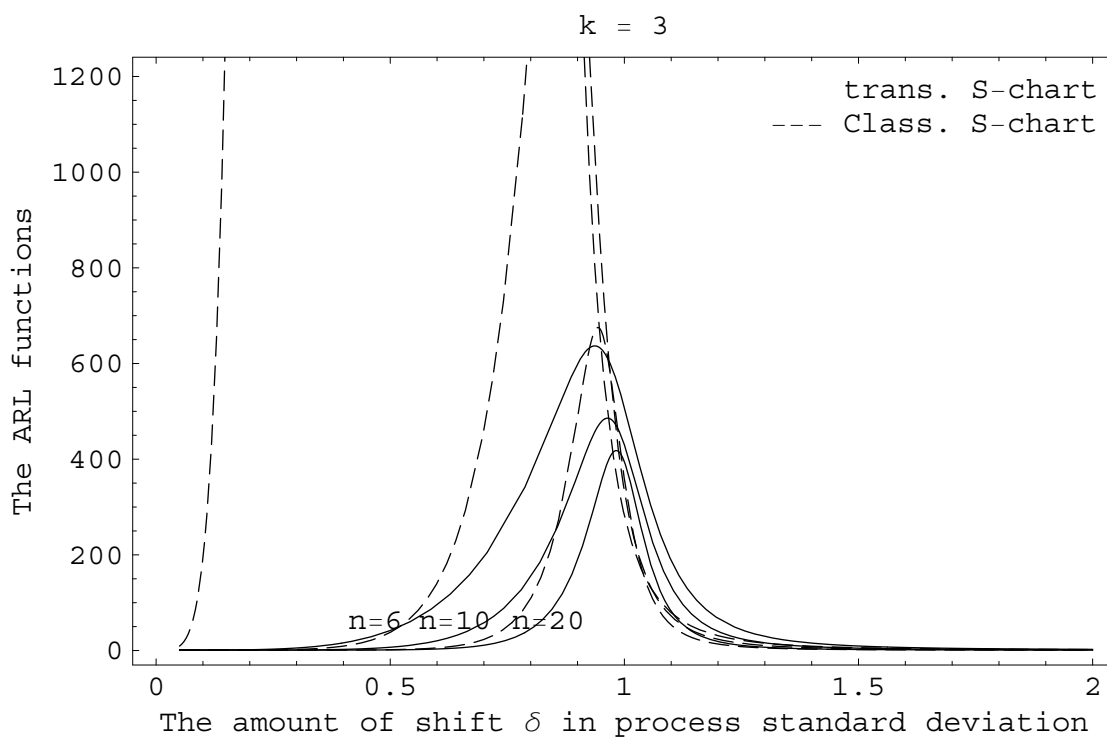
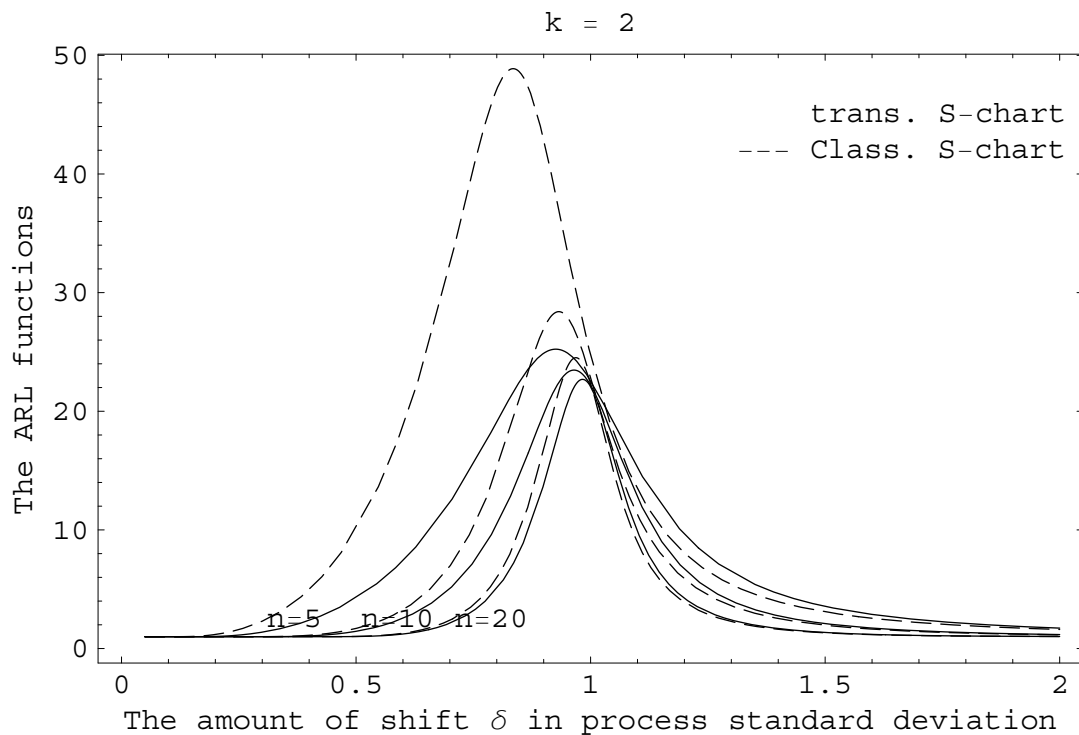


Figure 6: Plots of ARL Functions:  $m = \infty$

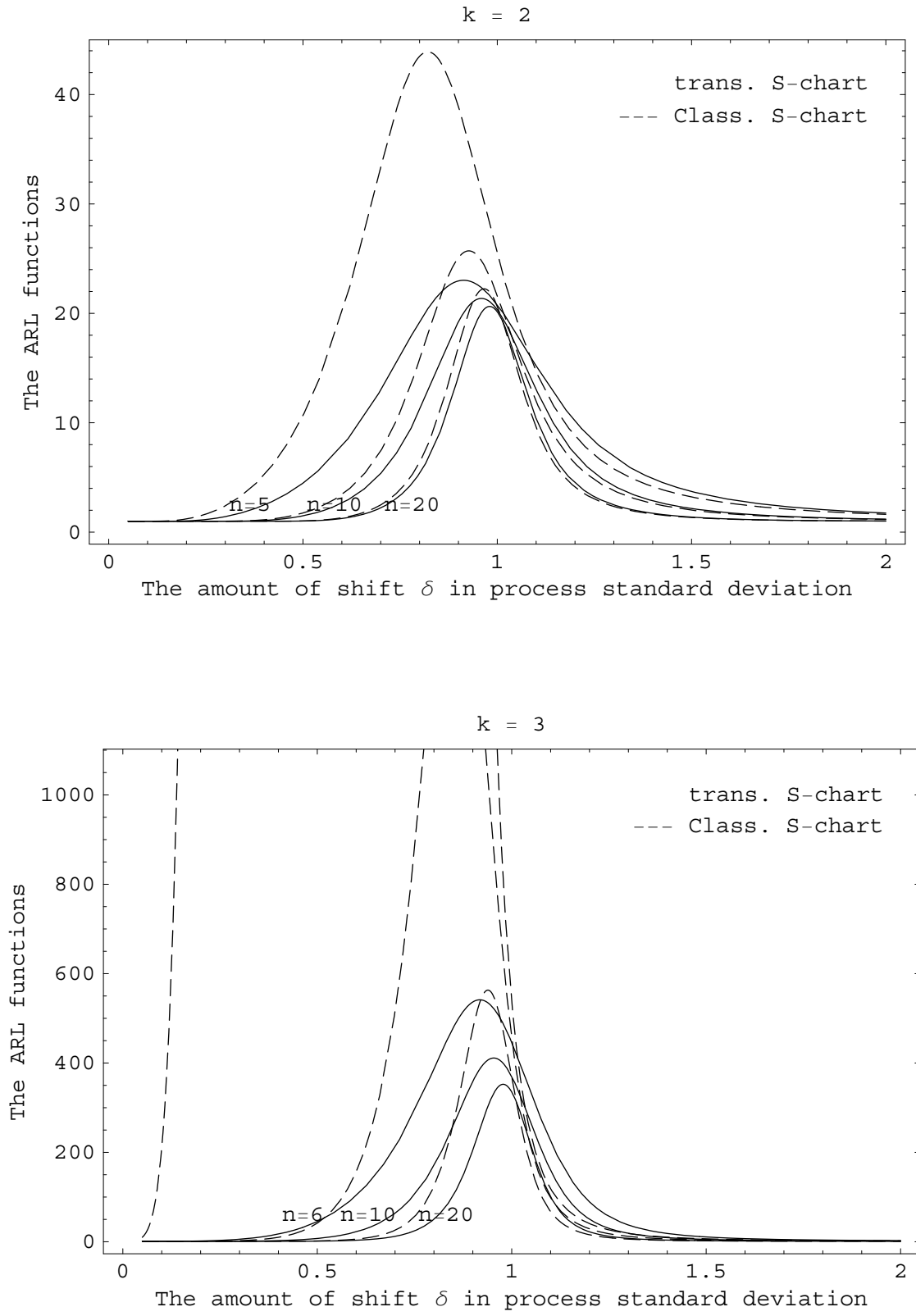


Figure 7: Plots of ARL Functions:  $m = 20$

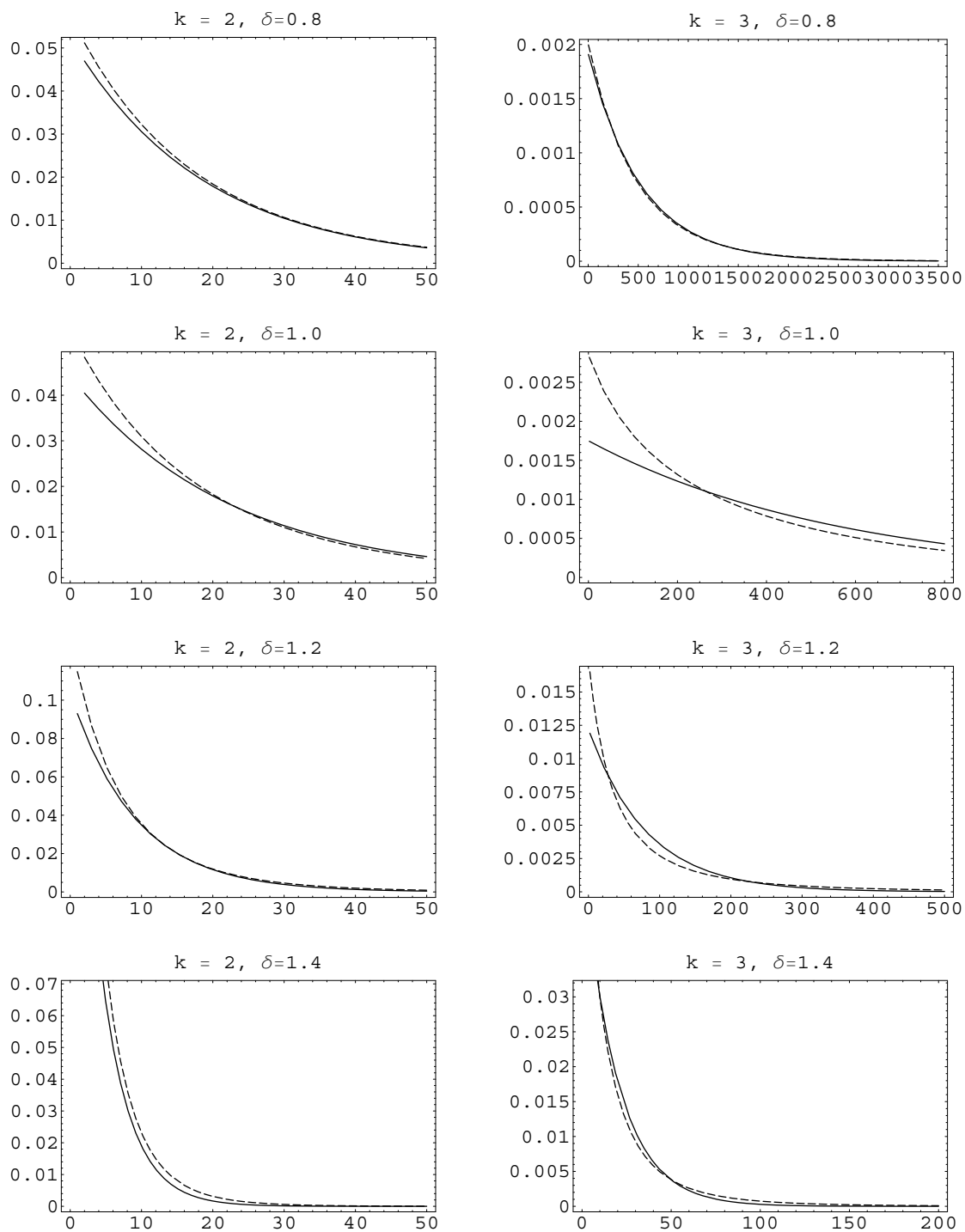


Figure 8: RL Distributions for the Transformation S-Chart with  $n = 5$  and  $m = 20$ .

With the help of Table 1, the construction of the transformation  $S$ -chart remains fairly simple, as compared with the classical  $S$ -chart. Woodall and Montgomery (1999) review the research issues and ideas in statistical process control and Elsayed (2000) summarizes the recent advances in the quality and reliability engineering methodologies.

It should be pointed out that a critique against using transformation is that the transformed data may not have any physical meaning as they are not direct measurement. However, such a problem is less serious for  $S$ -chart as  $S$  values are not physical measurement to begin with. On the other hand, when the transformation technique is used, we can easily transform the limits back to original scale although such approach will not lead to asymmetric limits. Such an approach is suitable when symmetric limits are not required and exact probability limits are not available.

## Appendix: A Normalizing Transformation for Gamma Distribution

We now give a brief description of the method for transforming the gamma variable to near normality. Let  $X$  be a gamma random variable with probability density function (pdf)  $f(x; \tau, \theta) = \Gamma^{-1}(\tau)\theta^{-\tau}x^{\tau-1}\exp(-x/\theta)$ . Let  $Y = X^\lambda$  and  $g(y; \tau, \theta, \lambda)$  be its pdf. Let  $\phi(y; \mu, \sigma)$  be the pdf of a normal random variable with mean  $\mu$  and standard deviation  $\sigma$ . Our aim is to find a  $\lambda$  value such that  $g(y; \tau, \theta, \lambda)$  and  $\phi(y; \mu, \sigma)$  are closest in the sense that the Kullback-Leibler (KL) information number (Kullback, 1968):

$$I(g, \phi) = \int_0^\infty g(y; \tau, \theta, \lambda) \log \left\{ \frac{g(y; \tau, \theta, \lambda)}{\phi(y; \mu, \sigma)} \right\} dy \quad (9)$$

is minimized with respect to  $\mu, \sigma$  and  $\lambda$ . For a given  $\lambda$ ,  $I$  is minimized at

$$\mu(\lambda) = E(Y) = \theta^\lambda \frac{\Gamma(\tau + \lambda)}{\Gamma(\tau)} \text{ and } \sigma^2(\lambda) \text{Var}(Y) = \theta^{2\lambda} \left[ \frac{\Gamma(\tau + 2\lambda)}{\Gamma(\tau)} - \frac{\Gamma^2(\tau + \lambda)}{\Gamma^2(\tau)} \right].$$

Substituting  $\mu(\lambda)$  and  $\sigma(\lambda)$  back into (15) gives the partially minimized KL number

$$\begin{aligned} I(\lambda) &= \frac{1}{2} [\log(2\pi) + 1] + 2 \log \Gamma(\tau) - \tau[\Psi(\tau) - 1] - \lambda\Psi(\tau) \\ &\quad + \frac{1}{2} \log \left[ \Gamma(\tau)\Gamma(\tau + 2\lambda) - \Gamma^2(\tau + \lambda) \right] - \log(\lambda) \end{aligned} \quad (10)$$

where  $\Gamma(\cdot)$  is the gamma function and  $\Psi(\cdot) = d \log \Gamma(x)/dx$  is the digamma function (Hernandez and Johnson, 1981). The optimal transformation parameter is obtained by minimizing (10) with respect to  $\lambda$  which is equivalent to solving the following equation:

$$G(\lambda) = \left[ \frac{\Gamma(\tau)\Gamma(\tau + 2\lambda)\Psi(\tau + 2\lambda) - \Gamma^2(\tau + \lambda)\Psi(\tau + \lambda)}{\Gamma(\tau)\Gamma(\tau + 2\lambda) - \Gamma^2(\tau + \lambda)} \right] - \frac{1}{\lambda} - \Psi(\tau) = 0. \quad (11)$$

The optimal transformation parameter depends only on the shape parameter  $\tau$ , and can be easily found using Mathematica with the following commands:

```

τ = 2;
g[λ_] :=  $\frac{\text{Gamma}[\tau]\text{PolyGamma}[\tau + 2\lambda] - \text{Gamma}[\tau + \lambda]^2\text{PolyGamma}[\tau + \lambda]}{\text{Gamma}[\tau]\text{Gamma}[\tau + 2\lambda] - \text{Gamma}[\tau + \lambda]^2} + \frac{1}{\lambda} - \text{PolyGamma}[\tau]$ 
FindRoot[g[λ] == 0, {λ, 0.3}]

```

Changing the input value for  $\tau$  gives a different optimal transformation value  $\lambda_0$ . The corresponding  $\mu(\lambda_0)$  and  $\sigma(\lambda_0)$  can be easily calculated by Mathematica.

## References

- ACOSTA-MEJIA, C. A., PIGNATIELLO, J.J. JR. and RAO, B. V. (1999). A Comparison of Control Charting Procedures for Monitoring Process Dispersion, *IIE Transactions*, 31, pp. 569-579.
- CHAKRABORTI, S. (2000). Run Length, Average Run Length and False Alarm Rate of Shewhart X-bar Chart: Exact Derivation by Conditioning, *Communications in Statistics—Simulation and Computation*, 29, pp. 61-68.
- CHEN, G. (1998). The Run Length Distributions of the  $R$ ,  $s$  and  $s^2$  Control Charts when  $\sigma$  is Estimated, *The Canadian Journal of Statistics*, 26, pp. 311-322.
- CHOW, Y.-M., POLANSKY, A. M. and MASON, R. L (1998). Transforming Non-Normal Data to Normality in Statistical Process Control, *Journal of Quality Technology*, 30, pp. 133-141.
- ELSAIED, E. A. (2000). Perspectives and Challenges for Research in Quality and Reliability Engineering, *International Journal of Production Research*, 38, pp. 1953-1976.

- HAWKINS, D. M. and WIXLEY, R. A. J. (1986). A Note on the Transformation of Chi-Squared Variables to Normality, *The American Statistician*, 40, pp. 296-298.
- HERNANDEZ, F. and JOHNSON, R. A. (1981). The Large Sample Behavior of Transformations to Normality, *Journal of the American Statistical Association*, 75, pp. 855-861.
- KITTLITZ, R. G. JR. (1999). Transforming the Exponential for SPC Applications, *Journal of Quality Technology*, 31, pp. 301-308.
- KULLBACK, S. (1968). *Information Theory and Statistics*, New York: Dover Publications.
- LOWRY, C. A., CHAMP, C. W. and WOODALL, W. H. (1995). The Performance of Control Charts for Monitoring Process Variation, *Communications in Statistics-Simulation and Computation*, 24, pp. 409-437.
- MONTGOMERY, D. C. (1997). *Introduction to Statistical Quality Control*, 3rd ed. John Wiley & Sons, New York, NY.
- NELSON, L. S. (1984). The Shewhart Control Chart-Tests for Special Causes, *Journal of Quality Technology*, 16, pp. 237-239.
- NELSON, L. S. (1994). A Control Chart for Parts-Per-Million Nonconforming Items, *Journal of Quality Technology*, 26, pp. 239-240.
- PPARKHIDEH, S. and PPARKHIDEH, B. (1996). Economic Design of a Flexible Zone  $\bar{X}$ -Chart with AT&T Rules, *IIE Transactions*, 28, pp. 261-266.
- QUESENBERY, C. P. (1997). *SPC Methods for Quality Improvement*, John Wiley & Sons, New York, NY.
- SHORE, H. (2000a). General Control Charts for Variables, *International Journal of Production Research*, 30, pp. 1875-1897.
- SHORE, H. (2000b). General Control Charts for Attributes, *IIE Transactions*, 30, pp. 1875-1897.



WESTERN ELECTRIC (1956). *Statistical Quality Control Handbook*, Western Electric Corporation, Indianapolis, Indiana, USA.

WOODALL, W. H. and MONTGOMERY, D. C. (1999). Research Issues and Ideas in Statistical Process Control, *Journal of Quality Technology*. 31, pp. 376-386.

XIE M., GOH T.N., TANG, X.Y. (2000). Data Transformation for Geometrically Distributed Quality Characteristics, *Quality and Reliability Engineering International*. 16, pp 9-15.

YANG Z. and XIE X. (2000). Process monitoring of exponentially distributed characteristics through an optimal normalizing transformation, *Journal of Applied Statistics*, 27, 1051-1063.